

ESSAM: A Novel Competitive Evolution Strategies Approach to Reinforcement Learning for Memory Efficient LLMs Fine-Tuning

Zhishen Sun^{* 1} Sizhe Dang^{* 1} Guang Dai² Haishan Ye^{1,2}

Abstract

Reinforcement learning (RL) has become a key training step for improving mathematical reasoning in large language models (LLMs), but it often has high GPU memory usage, which makes it hard to use in settings with limited resources. To reduce these issues, we propose Evolution Strategies with Sharpness-Aware Maximization (ESSAM), a full parameter fine-tuning framework that tightly combines the zero-order search in parameter space from Evolution Strategies (ES) with the Sharpness-Aware Maximization (SAM) to improve generalization. We conduct fine-tuning experiments on the mainstream mathematical reasoning task GSM8K. The results show that ESSAM achieves an average accuracy of 78.27% across all models and its overall performance is comparable to RL methods. It surpasses classic RL algorithm PPO with an accuracy of 77.72% and is comparable to GRPO with an accuracy of 78.34%, and even surpassing them on some models. In terms of GPU memory usage, ESSAM reduces the average GPU memory usage by 18 \times compared to PPO and by 10 \times compared to GRPO, achieving an extremely low GPU memory usage.

1. Introduction

Recent breakthroughs in the mathematical reasoning ability of large language models (LLMs) have led to their deep integration with many scientific fields such as mathematics and physics, making them an indispensable part of modern life (Guo et al., 2025; Yang et al., 2025; OpenAI, 2025; Comanici et al., 2025). These gains in mathematical reasoning are largely driven by the rise of Reinforcement learning (RL) as a fine-tuning method (Schulman et al., 2017; Shao et al., 2024; Yu et al., 2025; Zheng et al., 2025). However, despite its effectiveness, applying RL to fine-tune LLMs requires extremely high GPU memory resources (Dong et al., 2024),

¹Xi'an Jiaotong University ²SGIT AI Lab. Correspondence to: Haishan Ye <yehaishan@xjtu.edu.cn>.

such as fine-tuning an 8B model with PPO, 314.44 GiB of GPU memory is required (Appendix D), which is not friendly to resource constrained open-source communities, and limits the further development of using RL to fine-tune LLMs.

To mitigate the issue that RL requires extremely high GPU memory resources, Qiu et al. (2025) explore using Evolution Strategies (ES) to fine-tune LLMs. ES is a population based zero-order method, which does not rely on gradients and updates model parameters using only forward generation and reward evaluation. Therefore, ES can significantly reduce GPU memory usage and training cost. However, on mainstream mathematical reasoning tasks such as GSM8K (Cobbe et al., 2021), the overall performance of ES is often limited and difficult to match the performance of RL methods. The reason lies in the fact that ES only explores within the model's parameter space and then directly updates the parameters. This update approach tends to drive the model toward sharp minima, resulting in poor generalization performance. In addition, in their ES experiments, Qiu et al. (2025) use only 200 examples for training and 2,000 examples for evaluation. This split is not a standard setup, and during training the 200 examples are used as a whole without the common practice of shuffling the training data and iterating with small mini batches. This can introduce more randomness and differs from standard LLMs fine-tuning pipelines. So the practical performance of ES still needs further study.

Recent work on Sharpness-Aware Minimization (Maximization) has shown strong gains in generalization (Foret et al., 2020). Its key idea is to reduce both the loss value and the loss sharpness, so that training moves toward flat minima where the loss stays low in a whole neighborhood of the parameters. This can reduce overfitting and make the model more robust. We introduce the idea of SAM into zeroth-order search and propose a new zeroth-order fine-tuning method called Evolution Strategies with Sharpness-Aware Maximization (ESSAM). As shown in Figure 1, ESSAM tightly integrates the sharpness-aware perturbation mechanism of SAM with ES, it uses the update direction that would otherwise move the original parameters toward sharp regions to perform a reverse update, obtains a new update

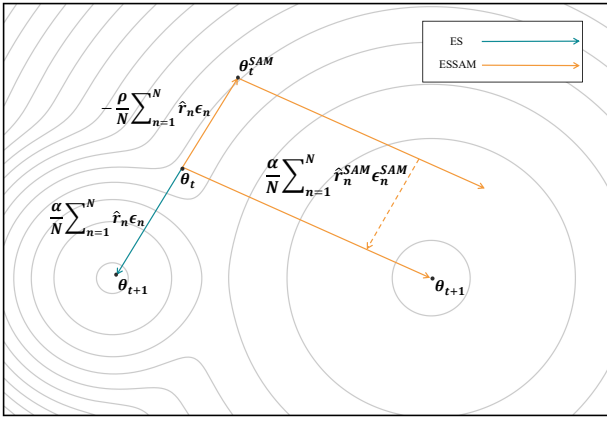


Figure 1. An illustration of the ESSAM parameter update.

direction at the perturbed parameters, and then uses this new direction to update the original parameters, so that the solution of the model is guided to converge to flatter regions, enhancing the model’s robustness and generalization ability.

We follow a more standard training procedure. We use a standard split between training data and evaluation data, shuffle the training data, and perform multi step updates with small mini batches, rather than training once on a small set of samples as a whole. This reduces randomness from small sample training and better averages the noise induced variation across iterations, and the training signal is smoother and the optimization process is more stable.

Experimental results show that ESSAM extends ES to the mainstream mathematical reasoning task GSM8K and substantially improves the generalization of LLMs. While keeping low GPU memory usage, ESSAM performs much better than standard ES on the GSM8K task. It matches the strong RL methods PPO and GRPO (Figure 2), and it even surpasses them on some models (refer to Table 1). These results indicate improved generalization and highlight the advantages and potential of ESSAM as a zero-order method for fine-tuning LLMs. We summarize contributions as follows:

- We propose a new zero-order full parameter fine-tuning framework ESSAM, which introduces neighborhood probing and a two stage evaluation update in parameter space, and guides optimization toward flatter and more robust solutions. *ESSAM achieves RL training performance while maintaining inference-level GPU memory usage.*
- We extend the zero-order fine-tuning framework to the mainstream mathematical reasoning task GSM8K for the first time. We also adopt a more standard data

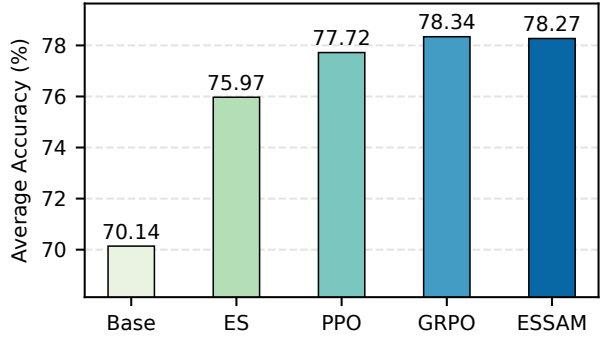


Figure 2. The average accuracy of each algorithm on all models for the GSM8K task (%).

usage and training procedure, including a standard split of training and evaluation sets, shuffling the training data, and performing multi step updates with small mini batches. This reduces randomness from small sample training and improves training stability and reproducibility.

- We conduct experiments on GSM8K, and the results show that ESSAM achieves an average accuracy of 78.27% across all models, significantly outperforming standard ES with 75.97%. Comparing to PPO’s 77.72% and GRPO’s 78.34%, ESSAM performs similarly and even surpasses them on some models. Further analysis indicates that ESSAM exhibits better training trends than standard ES and achieves higher test accuracy, demonstrating stronger generalization ability.
- We evaluate the GPU memory requirements and find that ESSAM maintains the same GPU memory usage as ES. On average, ESSAM reduces GPU memory usage by 18× compared to PPO and by 10× compared to GRPO, achieving an extremely low, inference-level GPU memory usage and greatly reducing the demand for computational resources.

2. Related Work

Evolution Strategies. ES is first developed for continuous numerical optimization. The basic idea is to create a population by adding random perturbations to candidate solutions, and then recombine these perturbed solutions based on their fitness to produce the next generation. Within this framework, classic methods such as CMA-ES (Hansen & Ostermeier, 2001) and Natural Evolution Strategies (Wierstra et al., 2014) were proposed, which later laid the foundation for using evolutionary search to optimize neural network parameters. In Transformer and LLMs settings, search-

ing over billions of parameters with evolutionary methods was long considered hard, so early work mainly focused on small scale or parameter efficient subspaces. For example, [Toledano-López et al. \(2022\)](#) used CMA-ES to fine tune only a small last layer of an mT5 model, and [Jin et al. \(2024\)](#) optimized LoRA low rank adapter parameters using CMA-ES and the Fireworks algorithm. [Carmona et al. \(2024\)](#) explored using a genetic algorithm to fine tune a larger number of parameters in a Transformer encoder, but its overall results were usually weaker than the Adam optimizer. More recently, [Qiu et al. \(2025\)](#) make engineering and parallelization advances that scale ES to full parameter search in billion parameter LLMs. Although their generalization is still limited and do not transfer well to mainstream math reasoning tasks, their successful practices have provided important inspiration for our work.

Reinforcement learning. RL fine-tuning is an important method for improving the performance of LLMs ([Christiano et al., 2017](#); [Ziegler et al., 2019](#); [Ouyang et al., 2022](#)) and their mathematical reasoning ability ([Guo et al., 2025](#)), and it has become a key step in the training pipelines of leading LLMs. PPO ([Schulman et al., 2017](#)) and GRPO ([Shao et al., 2024](#)) are currently mainstream methods for RL training of LLMs. PPO stabilizes updates by using a clipped surrogate objective to limit the change in the ratio between the new and old policies, and it often combines a value function baseline and advantage estimation to reduce variance. GRPO is often viewed as an efficient variant of PPO. It removes the need for a value model of comparable size to the policy, and instead uses group scores from multiple sampled outputs under the same prompt as a baseline, together with relative advantage normalization, which can reduce resource cost. Although these RL methods have advantages in different respects and can significantly improve LLMs performance, they still consume substantial GPU memory resources.

Sharpness-Aware Minimization (Maximization). SAM ([Foret et al., 2020](#)) can encourages the model to converge to flatter minima and improves generalization. In the language model setting, prior work shows that sharpness aware training can reduce overfitting and improve downstream performance, and it also explores selective perturbations based on parameter importance. [Zhong et al. \(2022\)](#) propose a Fisher information based mask to balance stability and gains. [Liu et al. \(2022\)](#) reduce the extra cost of SAM by changing the perturbation and update procedure from an efficiency and scalability perspective, making it more suitable for large scale training. When gradients are unavailable or only forward passes can be used, [Ye et al. \(2024\)](#) introduce sharpness aware ideas into black box optimization through a distribution based reparameterization and provides theoretical analysis. [Fu et al. \(2025\)](#) propose ZOSA is a novel zero-order sharpness-aware minimization framework that integrates Rademacher perturbations and adaptive

loss-variance scaling to enable efficient prompt tuning for LLMs. Inspired by this work, we extend the idea of combining zeroth-order fine-tuning with SAM to the ES setting and apply it to improve the mathematical reasoning ability of LLMs.

3. Method

In this section, we detailed introduction the algorithm flow (Sec. 3.1) and efficient memory saving mechanism (Sec. 3.2) of our proposed ESSAM algorithm. Finally, we explain why our proposed algorithm can be viewed as performing Sharpness-Aware Maximization (Sec. 3.3).

3.1. Evolution Strategies with Sharpness-Aware Maximization

ES generates a population of perturbation models with Gaussian noise and updates parameters in a reward-weighted manner, exploring and updating the parameter space only once in each iteration (Appendix A). Different from standard ES, our ESSAM method introduces the SAM mechanism. It first uses the current reward weighted aggregation to move the model parameters in the opposite direction of reward increase to a nearby neighborhood point, and then uses the perturbations and rewards computed at this point to update the parameters. This process helps avoid sharp solutions and drives the model toward flatter and more robust regions, thereby improving generalization.

Specifically, given a pretrained LLM with parameters θ_0 and a reward function $R(\theta)$, we aim to maximize the expected reward by iteratively updating model parameters. At iteration t , we sample N i.i.d. Gaussian noises $\epsilon_n \sim \mathcal{N}(0, I)$ for $n = 1, \dots, N$, and construct perturbed models:

$$\theta_t^{(n)} = \theta_t + \sigma \epsilon_n, \quad n = 1, \dots, N. \quad (1)$$

We evaluate each perturbed model to obtain reward scores:

$$r_n = R(\theta_t^{(n)}), \quad n = 1, \dots, N. \quad (2)$$

We then apply z-score normalization ([Qiu et al., 2025](#)) to keep the reward scale consistent:

$$\mu_r = \frac{1}{N} \sum_{n=1}^N r_n, \quad s_r = \sqrt{\frac{1}{N-1} \sum_{n=1}^N (r_n - \mu_r)^2}, \quad (3)$$

$$\hat{r}_n = \frac{r_n - \mu_r}{s_r + \delta}, \quad n = 1, \dots, N, \quad (4)$$

where δ is a small constant for numerical stability.

Next, different from standard ES, which directly updates parameters using \hat{r}_n , we use \hat{r}_n to compute a weighted aggregation of the corresponding noise directions. This

Algorithm 1 Evolution Strategies with Sharpness-Aware Maximization (ESSAM)

Input: initial parameters θ_0 , reward function R , population size N , noise scale σ , hyperparameter ρ , learning rate α , iterations T , number of parallel processes P

Output: fine-tuned parameters θ_T

Create P processes, each instantiates a model with the same initial parameters θ_0 , with one process as the main process

for $t = 0$ **to** $T - 1$ **do**

- (Stage 1) **Build a SAM neighborhood point** θ_t^{SAM}
 - Sample N random seeds s_1, \dots, s_N
 - $\{r_n\}_{n=1}^N \leftarrow SRE(\theta_t, R, \sigma, \{s_n\}_{n=1}^N, P)$
 - Compute mean μ_r , std s_r
 - Normalize $\hat{r}_n = \frac{r_n - \mu_r}{s_r + \delta}$
 - $\theta_t^{\text{SAM}} \leftarrow DIPU(\theta_t, \{s_n\}_{n=1}^N, \{\hat{r}_n\}_{n=1}^N, -\rho)$
 - Broadcast parameters of all processes to θ_t^{SAM}
- (Stage 2) **Evaluate around** θ_t^{SAM} **and update** θ_t
 - Sample N random seeds $s_t^{\text{SAM}}, \dots, s_N^{\text{SAM}}$
 - $\{\hat{r}_n\}_{n=1}^N \leftarrow SRE(\theta_t^{\text{SAM}}, R, \sigma, \{s_n^{\text{SAM}}\}_{n=1}^N, P)$
 - Compute mean μ_r^{SAM} , std s_r^{SAM}
 - Normalize $\hat{r}_n^{\text{SAM}} = \frac{r_n^{\text{SAM}} - \mu_r^{\text{SAM}}}{s_r^{\text{SAM}} + \delta}$
 - $\theta_t \leftarrow DIPU(\theta_t^{\text{SAM}}, \{s_n\}_{n=1}^N, \{\hat{r}_n\}_{n=1}^N, \rho)$
 - $\theta_{t+1} \leftarrow DIPU(\theta_t^{\text{SAM}}, \{s_n^{\text{SAM}}\}_{n=1}^N, \{\hat{r}_n^{\text{SAM}}\}_{n=1}^N, \alpha)$
 - Broadcast parameters of all processes to θ_{t+1}

end for

Algorithm 2 Seed Replay Eval (SRE)

Input: parameters θ , reward function R , noise scale σ , seeds $\{s_n\}_{n=1}^N$, number of parallel processes P

Output: rewards $\{r_n\}_{n=1}^N$

Assign seeds $\{s_n\}_{n=1}^N$ to P processes for fully-parallel evaluations

for $n = 1$ **to** N **do**

- For the process handling s_n , reset its random number generator using seed s_n
- for** each LLM layer **do**

 - Using seed s_n , sample noise $\epsilon_{n,l} \sim \mathcal{N}(0, I)$
 - Perturb in-place: $\theta_l \leftarrow \theta_l + \sigma \epsilon_{n,l}$

- end for**
- Evaluate reward $r_n = R(\theta)$ using greedy decoding
- For the process handling s_n , reset its random number generator using seed s_n
- for** each LLM layer **do**

 - Using seed s_n , sample noise $\epsilon_{n,l} \sim \mathcal{N}(0, I)$
 - Restore in-place: $\theta_l \leftarrow \theta_l - \sigma \epsilon_{n,l}$

- end for**

end for

forms a combined perturbation for neighborhood probing, and we control its magnitude using the hyperparameter ρ , which perturbs the parameters from θ_t to a neighborhood

Algorithm 3 Decomposed In-place Update (DIPU)

Input: parameters θ , seeds $\{s_n\}_{n=1}^N$, weights $\{w_n\}_{n=1}^N$, step size η

Output: updated parameters θ

for $n = 1$ **to** N **do**

- For the process handling s_n , reset its random number generator using seed s_n
- for** each LLM layer **do**

 - Using seed s_n , sample noise $\epsilon_{n,l} \sim \mathcal{N}(0, I)$
 - Update in-place: $\theta_l \leftarrow \theta_l + \eta \cdot \frac{1}{N} w_n \epsilon_{n,l}$

- end for**

end for

point θ_t^{SAM} . The perturbation is given by:

$$\theta_{t+1}^{\text{SAM}} = \theta_t - \rho \cdot \frac{1}{\sigma} \frac{1}{N} \sum_{n=1}^N \hat{r}_n \epsilon_n. \quad (5)$$

Above operations are shown in the first stage of ESSAM shown in Algorithm 1.

After obtaining $\theta_{t+1}^{\text{SAM}}$, we sample another N i.i.d. Gaussian noises $\epsilon_n^{\text{SAM}} \sim \mathcal{N}(0, I)$ at $\theta_{t+1}^{\text{SAM}}$ and repeat the same steps of perturbation, evaluation, and z-score normalization, producing normalized rewards \hat{r}_n^{SAM} at $\theta_{t+1}^{\text{SAM}}$. Finally, we restore the parameters back to the original θ_t , and use \hat{r}_n^{SAM} together with their corresponding noise to form a weighted aggregation for the final update with learning rate α , where we have absorbed $1/\sigma$ into α :

$$\theta_{t+1} = \theta_t + \alpha \cdot \frac{1}{N} \sum_{n=1}^N \hat{r}_n^{\text{SAM}} \epsilon_n^{\text{SAM}}. \quad (6)$$

Above operations are shown in the second stage of ESSAM shown in Algorithm 1.

3.2. Memory Saving Mechanism

To make ESSAM practical for fine-tuning LLMs, we adopt the memory saving techniques proposed by Qiu et al. (2025) to reduce GPU memory usage during training. The detailed implementation is shown in Algorithms 2 and 3.

Both stages of ESSAM use these memory saving techniques. Together with the zero-order update that relies on forward generation and reward evaluation rather than backpropagation, ESSAM greatly reduces GPU memory usage and avoids the high memory cost seen in RL methods.

Algorithm 1 shows the detailed procedure of ESSAM.

3.3. Understanding the algorithm design of ESSAM

In the SAM setting, when constructing the SAM neighborhood point in the first stage, its structural form is as follows

(Foret et al., 2020):

$$\theta_{t+1}^{\text{SAM}} = \theta_t - \rho \cdot \frac{g}{\|g\|}, \quad (7)$$

Where g is a gradient direction.

In our setting, the gradient estimate is computed as:

$$g_t = \frac{1}{\sigma} \frac{1}{N} \sum_{n=1}^N (r_n - \mu_r) \epsilon_n, \quad (8)$$

The estimated variance s_r^2 is computed as:

$$s_r^2 = \frac{1}{N-1} \sum_{n=1}^N (r_n - \mu_r)^2, \quad (9)$$

In our algorithm, the SAM neighborhood point is constructed as follows:

$$\theta_{t+1}^{\text{SAM}} = \theta_t - \rho \cdot \frac{g_t}{s_r}. \quad (10)$$

Proposition 3.1 shows why the first stage update of our proposed algorithm is essentially performing SAM.

Proposition 3.1. *Let the stochastic gradient estimation g_t defined in Eq. (8) and the variance s_r^2 defined in Eq. (9). Then it holds that*

$$\mathbb{E}[g_t] = \frac{N-1}{N} \nabla R(\theta) + \tau, \quad \tau = O(\sigma) \quad (11)$$

$$\begin{aligned} \mathbb{E}[\|g_t\|^2] &= \frac{N^3 + (d-2)N^2 + (3-2d)N + d-2}{N^3} \\ &\quad \cdot \|\nabla R(\theta)\|^2 + \gamma, \quad \gamma = O(\sigma). \end{aligned} \quad (12)$$

$$\mathbb{E}[s_r^2] = \sigma^2 \|\nabla R(\theta)\|^2 + \zeta, \quad \zeta = O(\sigma^3). \quad (13)$$

$$\begin{aligned} \mathbb{E}[\|g_t\|^2] &\approx \frac{N^3 + (d-2)N^2 + (3-2d)N + d-2}{N^3} \cdot \sigma^{-2} \\ &\quad \cdot \mathbb{E}[s_r^2]. \end{aligned} \quad (14)$$

where d denotes the number of model parameters.

Detailed proof of Proposition 3.1 is in Appendix B.

Since $\frac{N^3 + (d-2)N^2 + (3-2d)N + d-2}{N^3} \cdot \sigma^{-2}$ is a constant, $\frac{g_t}{s_r}$ and $\frac{g_t}{\|g_t\|}$ can be regarded as equivalent, scaled only by a constant factor. Therefore, the first stage update of our proposed algorithm is essentially performing Sharpness-Aware Maximization.

4. Experiment

We conduct experiments on a mainstream mathematical reasoning task GSM8K. Section 4.1 introduces the experimental setup. Section 4.2 presents the detailed results (Sec. 4.2.1) and provides an analysis of GPU memory usage and computational efficiency (Sec. 4.2.2).

4.1. Experimental Setup

Models. In our experiments, we train the following models.

- **Qwen:** Qwen-2.5-0.5B-Instruct, Qwen-2.5-1.5B-Instruct, Qwen-2.5-3B-Instruct, Qwen-2.5-7B-Instruct;
- **Llama:** LLaMA-3.2-1B-Instruct, LLaMA-3.2-3B-Instruct, LLaMA-3.1-8B-Instruct.

Datasets. In our experiments, we use the GSM8K dataset to train and evaluate LLMs. This task mainly tests text understanding, multi step reasoning, and arithmetic computation. The problem and prompt template are shown in Figure 3.

Problem: Natalia sold clips to 48 of her friends in April, and then she sold half as many clips in May. How many clips did Natalia sell altogether in April and May?

Template: You are a helpful assistant. You first think about the reasoning process in your mind and then provide the user with the answer.

Please solve the following problem: {question}
Show your work in <think> </think> tags.
And put the final numerical answer after #####.

Figure 3. An example GSM8K problem and the prompt template.

Reward function. For verifiable math reasoning tasks such as GSM8K and Countdown, we use a rule based reward function. The rules are as follows, we split the reward into an outcome accuracy reward and an output format reward:

$$R_{\text{accuracy}}(\hat{y}, y) = \begin{cases} 1, & \text{is_equivalent}(\hat{y}, y), \\ 0, & \text{otherwise.} \end{cases} \quad (15)$$

$$R_{\text{format}}(a) = \begin{cases} 1.0, & \text{the output follows the full format;} \\ 0.6, & \text{it contains both a } \textit{thinking marker} \\ & \text{and an } \textit{answer marker}; \\ 0.1, & \text{it contains a } \textit{thinking marker} \text{ only;} \\ 0.5, & \text{it contains an } \textit{answer marker} \text{ only;} \\ 0.0, & \text{otherwise.} \end{cases} \quad (16)$$

Table 1. Accuracy of different algorithms on different models and average accuracy for the GSM8K task (%).

METHOD	QWEN-2.5-INSTRUCT				LLAMA-INSTRUCT			AVERAGE
	0.5B	1.5B	3B	7B	3.2-1B	3.2-3B	3.1-8B	
ORIGINAL	46.47	73.77	84.84	90.52	39.04	74.60	81.73	70.14
PPO	53.90	78.85	87.19	91.28	61.49	83.02	88.29	77.72
GRPO	54.24	78.39	87.34	93.02	62.32	84.00	89.08	78.34
ES	52.46	75.97	86.66	90.98	57.24	80.97	87.54	75.97
ESSAM(OURS)	54.06	78.92	87.71	92.57	61.79	83.93	88.93	78.27

The final reward we use is a weighted sum of the accuracy reward and the format reward:

$$R(a, y) = R_{\text{answer}}(\hat{y}, y) + 0.1 R_{\text{format}}(a), \quad (17)$$

where y is the ground truth answer, \hat{y} is the model predicted answer, and a is the full model response to the question.

Hyperparameter setting. For each algorithm, we tune its hyperparameters and report the best performing setting. The detailed hyperparameter values are provided in Appendix C.

4.2. Experimental Results

4.2.1. MAIN RESULTS

On the mainstream mathematical reasoning task GSM8K, ESSAM significantly improves the performance of all tested models and achieves performance on par with mainstream RL methods. On the mainstream mathematical reasoning benchmark GSM8K, we systematically compare the fine-tuning performance of our proposed ESSAM with ES, PPO, and GRPO across base models of different sizes and architectures, as shown in Table 1. Overall, ESSAM delivers consistent gains on all models and raises the overall performance of zeroth-order fine-tuning to a level that is nearly comparable to mainstream RL methods. The average accuracy of ESSAM reaches 78.27%, which is significantly higher than the base models at 70.14%, representing an improvement of 8.13%, and it is also clearly better than standard ES at 75.97%, providing an additional gain of 2.3%. Moreover, ESSAM achieves average performance on par with RL methods, its average accuracy surpasses PPO at 77.71% and is essentially comparable to GRPO at 78.34%.

More specifically, on the Qwen 2.5 family, ESSAM achieves the best results on the 1.5B and 3B models, reaching 78.92% and 87.71% accuracy respectively, both higher than PPO and GRPO. On the 0.5B model, ESSAM is only 0.18% lower than GRPO, and it is higher than PPO with 53.90% accuracy. On the 7B model, ESSAM remains competitive with RL methods and reaches 92.57%, outperforming PPO. On the LLaMA family, ESSAM is also stable. It achieves 61.79%, 83.93%, and 88.93% accuracy on LLaMA-3.2-1B-it, LLaMA-3.2-3B-it, and LLaMA-3.1-8B-it respectively,

which are comparable to GRPO and all higher than PPO. These results further indicate that the advantage of ESSAM is not concentrated on a single model or a specific scale. Instead, it is consistent across different model families, and it remains stable from small models to medium and large models, suggesting strong cross model generalization and good transferability. In contrast, while standard ES can bring some gains for LLMs, its improvements are less consistent, and it lags behind PPO and GRPO in both average accuracy and per model accuracy. Overall, these results show that ESSAM effectively alleviates the generalization weakness of standard ES on natural language math word problems. It makes zeroth-order full parameter fine-tuning competitive with RL on mainstream tasks such as GSM8K, and it expands the practical applicability of evolution strategy based fine-tuning for LLMs mathematical reasoning.

ESSAM shows stronger generalization than standard ES. In this experiment, we only compare our ESSAM method with standard ES and analyze the relation between the training process and the test results. During training, we record the average reward on the training data at each iteration to describe the convergence trend. Figure 4 shows the training reward curves of ESSAM and ES. It can be observed that the reward trends on the training set are very similar, with comparable curve shapes, and ESSAM often achieves higher training rewards. However, the higher training reward does not imply that ESSAM gains its advantage by overfitting the training data at the expense of test performance. On the contrary, the test results in Table 1 show that under the same settings, ESSAM achieves higher accuracy and consistently outperforms standard ES. This phenomenon suggests that ESSAM significantly improves the generalization ability of LLMs, encouraging them to learn more robust and flatter solutions during training, which leads to better performance on unseen samples.

4.2.2. GPU MEMORY USAGE AND TIME EFFICIENCY ANALYSIS

ESSAM can fine-tune LLMs using only inference-level GPU memory, greatly reducing GPU memory usage. In terms of GPU memory usage, we measure and compare the GPU memory usage across base models of different sizes

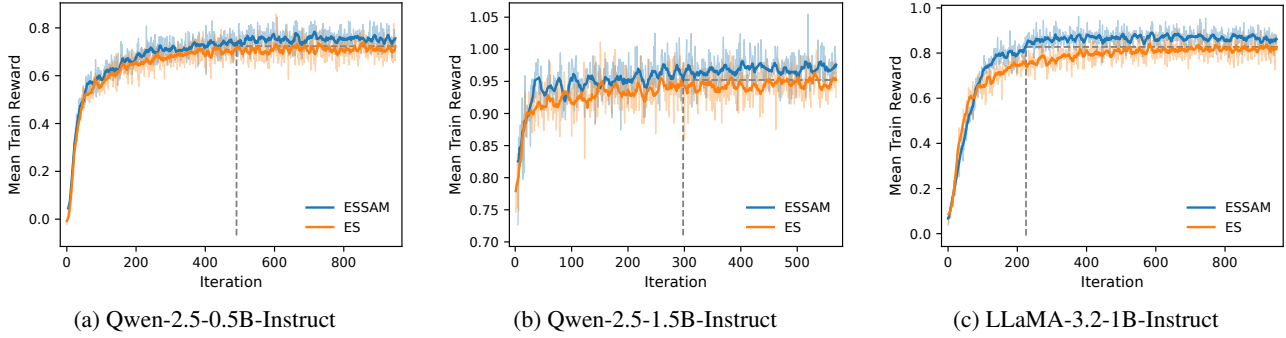


Figure 4. The training mean reward curves of ESSAM and ES. These curves show that ESSAM has better training trend and converges earlier than ES, leading to better computational efficiency. More results are presented in the Appendix E.

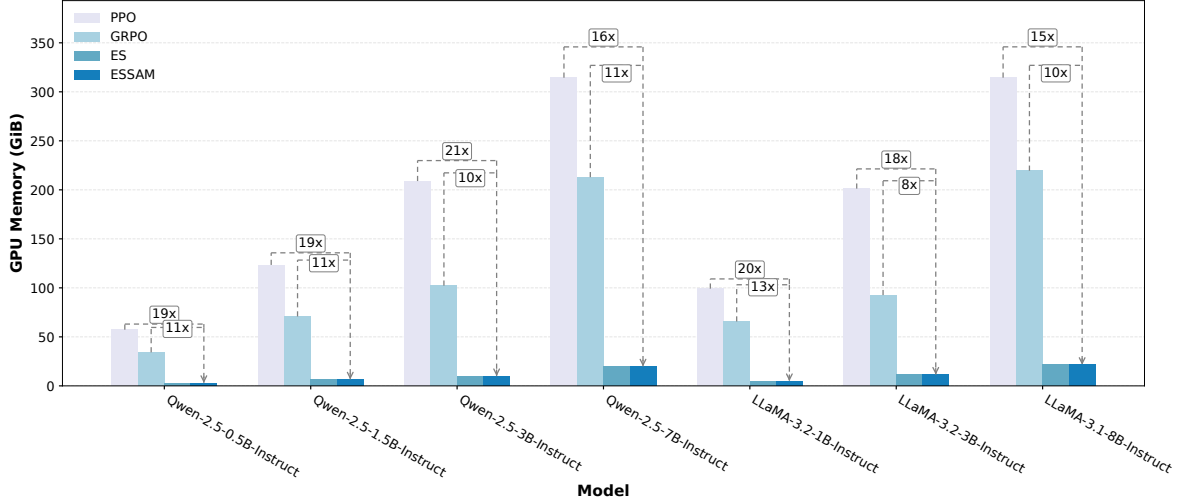


Figure 5. GPU memory usage when fine-tuning different LLMs with different algorithms. More details can be found in Appendix D.

and architectures on GSM8K, and the results in Figure 5 show a highly consistent and clear pattern. Across all models, ESSAM maintains the same extremely low, inference-level GPU memory usage as standard ES. This indicates that, with the aid of memory saving techniques, introducing the SAM mechanism, neighborhood probing and the two-stage evaluation update, into the ES framework does not lead to additional GPU memory usage. In contrast, the GPU memory usage of PPO and GRPO grows rapidly with model scale, often reaching hundreds of GiB for larger models, which is consistent with their reliance on backpropagation and policy updates, and their common use of KL control, a value network, and extra optimizer states. We further quantify this gap in Figure 5, comparing to PPO, ESSAM achieves about 15×–21× memory savings across models; compared to GRPO, it achieves about 8×–13× savings. On average, ESSAM reduces GPU memory usage by 18× compared to PPO and by 10× compared to GRPO, substantially lowering the demand for computational resources while preserving an inference-level GPU memory usage,

and making stable LLMs reasoning fine-tuning feasible in resource-constrained settings.

ESSAM has good time efficiency, and it shows a clear advantage in iteration efficiency compared to standard ES. As shown in Figure 4, for the training mean reward, ES can finally converge to a level close to ESSAM, but ESSAM reaches the reward value that ES only approaches near the end of training at a much earlier stage. ES needs almost the whole training process to reach the same level. This means that, under the same target reward, ESSAM needs far fewer iterations than ES to achieve a similar training result. In addition, Figure 6 shows how accuracy evolves with training progress. From the accuracy perspective, ESSAM can achieve fine-tuning performance on par with RL methods with no more than twice the training progress, or even with the same training progress as RL methods, whereas ES struggles to reach the RL level under the same training progress as ESSAM. Therefore, although ESSAM introduces neighborhood probing and a two stage evaluation update, which

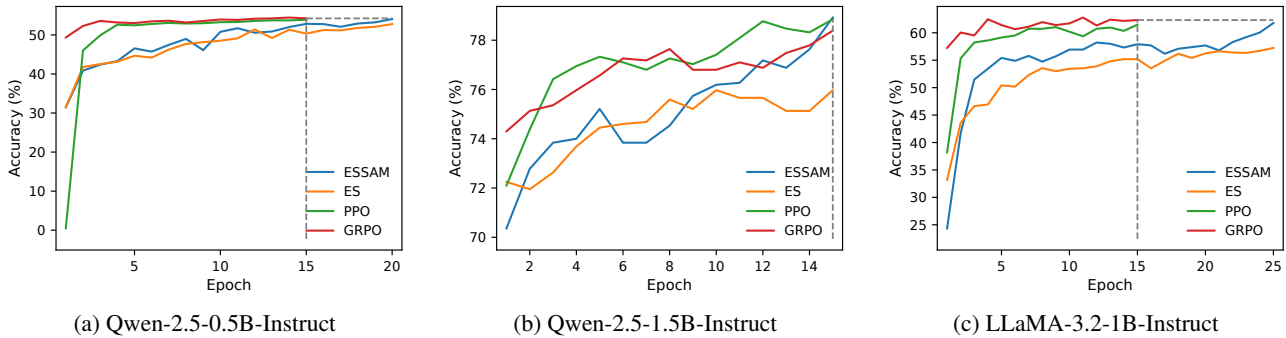


Figure 6. A schematic illustration of how the test set accuracy of models fine-tuned with different algorithms evolves over training. More results are shown in the Appendix F.

adds an extra round of sampling and reward evaluation in each iteration and slightly increases the per iteration time compared to ES, ESSAM converges much faster. This allows us to stop training earlier once the target reward is reached, so ESSAM has an advantage in total training time. This is also consistent with the design goal of ESSAM, the SAM helps the optimization reach flatter and more robust regions faster, which improves iteration efficiency and leads to better time efficiency in practice.

Table 2 reports the runtime of ESSAM and GRPO when fine-tuning different LLMs. In Table 2, on larger models such as Qwen-2.5-7B-Instruct, ESSAM runs faster and even reduces the runtime by nearly half compared to GRPO. Although ESSAM takes longer than GRPO on smaller models, the increase is not large. Except for Qwen-2.5-0.5B-Instruct, where ESSAM takes about 3.5 times the runtime of GRPO, the runtime of ESSAM on other models is approximately 2 times that of GRPO. This extra runtime is acceptable because ESSAM can achieve GRPO-level fine-tuning performance while using only inference-level GPU memory.

Discussion on the trade-off between memory and computation efficiency when using vLLM. During training, we use vLLM to accelerate inference. vLLM maintains a KV-cache to store key-value tensors of historical tokens, reducing redundant computations during the decoding phase, which enhances throughput and reduces latency. However, this comes with additional memory overhead, which increases with batch size, concurrency, and maximum generation length. By avoiding the need to store activations and gradients for backpropagation, ESSAM operates with memory usage close to inference-level. When memory is limited, the KV-cache usage can be controlled by reducing concurrency or maximum generation length to ensure stable training. When memory is sufficient, ESSAM can take advantage of available memory by increasing parallel request numbers or batch size, fully utilizing the KV cache to shorten the time needed for sampling and evaluation in each iteration, thus accelerating training.

Table 2. Training time when fine-tuning different LLMs with different algorithms.

BASE MODEL	GRPO	ESSAM
QWEN-2.5-0.5B-INSTRUCT	13.5	45
QWEN-2.5-1.5B-INSTRUCT	26.5	34
QWEN-2.5-3B-INSTRUCT	48	91
QWEN-2.5-7B-INSTRUCT	106	58.5
LLAMA-3.2-1B-INSTRUCT	19	33
LLAMA-3.2-3B-INSTRUCT	49	116
LLAMA-3.1-8B-INSTRUCT	105	233

5. Conclusion

In this paper, we propose ESSAM, a zero-order full parameter fine-tuning method that combines Evolution Strategies with the Sharpness-Aware Maximization mechanism, aiming to serve as an alternative to RL methods for improving the mathematical reasoning ability of LLMs under limited computational resources. ESSAM follows the zero-order training setting and relies only on forward generation and rule based reward evaluation. As a result, across different models, ESSAM maintains inference-level GPU memory usage, and its GPU memory usage is also significantly lower than that of PPO and GRPO. Experimental results show that ESSAM brings stable improvements on all models and clearly outperforms standard ES. It raises the overall performance to match PPO and GRPO, and it surpasses them on some models. Therefore, our work provides a practical and resource efficient option for math reasoning fine-tuning in settings with limited compute, and it also offers an additional feasible path for the open source community.

Impact Statement

This paper presents work whose goal is to advance the field of Machine Learning. There are many potential societal consequences of our work, none of which we feel must be specifically highlighted here.

References

Carmona, V. I. S., Jiang, S., and Dong, B. How well can a genetic algorithm fine-tune transformer encoders? a first approach. In *Proceedings of the Fifth Workshop on Insights from Negative Results in NLP*, pp. 25–33, 2024.

Christiano, P. F., Leike, J., Brown, T., Martic, M., Legg, S., and Amodei, D. Deep reinforcement learning from human preferences. *Advances in neural information processing systems*, 30, 2017.

Cobbe, K., Kosaraju, V., Bavarian, M., Chen, M., Jun, H., Kaiser, L., Plappert, M., Tworek, J., Hilton, J., Nakano, R., Hesse, C., and Schulman, J. Training verifiers to solve math word problems, 2021. URL <https://arxiv.org/abs/2110.14168>.

Comanici, G., Bieber, E., Schaeckermann, M., Pasupat, I., Sachdeva, N., Dhillon, I., Blstein, M., Ram, O., Zhang, D., Rosen, E., et al. Gemini 2.5: Pushing the frontier with advanced reasoning, multimodality, long context, and next generation agentic capabilities. *arXiv preprint arXiv:2507.06261*, 2025.

Dong, H., Xiong, W., Pang, B., Wang, H., Zhao, H., Zhou, Y., Jiang, N., Sahoo, D., Xiong, C., and Zhang, T. Rlfh workflow: From reward modeling to online rlfh, 2024. URL <https://arxiv.org/abs/2405.07863>.

Foret, P., Kleiner, A., Mobahi, H., and Neyshabur, B. Sharpness-aware minimization for efficiently improving generalization. *arXiv preprint arXiv:2010.01412*, 2020.

Fu, Y., Jin, Y., Zhang, C., Liu, J., and Ye, H. Zero-order sharpness-aware minimization. *arXiv preprint arXiv:2511.09156*, 2025.

Guo, D., Yang, D., Zhang, H., Song, J., Zhang, R., Xu, R., Zhu, Q., Ma, S., Wang, P., Bi, X., et al. Deepseek-r1: Incentivizing reasoning capability in llms via reinforcement learning. *arXiv preprint arXiv:2501.12948*, 2025.

Hansen, N. and Ostermeier, A. Completely derandomized self-adaptation in evolution strategies. *Evolutionary computation*, 9(2):159–195, 2001.

Jin, F., Liu, Y., and Tan, Y. Derivative-free optimization for low-rank adaptation in large language models. *IEEE/ACM Transactions on Audio, Speech, and Language Processing*, 2024.

Liu, Y., Mai, S., Chen, X., Hsieh, C.-J., and You, Y. Towards efficient and scalable sharpness-aware minimization. In *Proceedings of the IEEE/CVF Conference on Computer Vision and Pattern Recognition*, pp. 12360–12370, 2022.

OpenAI. O3 and o4 mini system card, 2025. URL <https://openai.com/index/o3-o4-mini-system-card/>.

Ouyang, L., Wu, J., Jiang, X., Almeida, D., Wainwright, C., Mishkin, P., Zhang, C., Agarwal, S., Slama, K., Ray, A., et al. Training language models to follow instructions with human feedback. *Advances in neural information processing systems*, 35:27730–27744, 2022.

Qiu, X., Gan, Y., Hayes, C. F., Liang, Q., Meyerson, E., Hodjat, B., and Miikkulainen, R. Evolution strategies at scale: Llm fine-tuning beyond reinforcement learning. *arXiv preprint arXiv:2509.24372*, 2025.

Schulman, J., Wolski, F., Dhariwal, P., Radford, A., and Klimov, O. Proximal policy optimization algorithms. *arXiv preprint arXiv:1707.06347*, 2017.

Shao, Z., Wang, P., Zhu, Q., Xu, R., Song, J., Bi, X., Zhang, H., Zhang, M., Li, Y., Wu, Y., et al. Deepseekmath: Pushing the limits of mathematical reasoning in open language models. *arXiv preprint arXiv:2402.03300*, 2024.

Toledano-López, O. G., Madera, J., González, H., Simón-Cuevas, A., Demeester, T., and Mannens, E. Fine-tuning mt5-based transformer via cma-es for sentiment analysis. In *IberLEF@ SEPLN*, 2022.

Wierstra, D., Schaul, T., Glasmachers, T., Sun, Y., Peters, J., and Schmidhuber, J. Natural evolution strategies. *The Journal of Machine Learning Research*, 15(1):949–980, 2014.

Yang, A., Li, A., Yang, B., Zhang, B., Hui, B., Zheng, B., Yu, B., Gao, C., Huang, C., Lv, C., et al. Qwen3 technical report. *arXiv preprint arXiv:2505.09388*, 2025.

Ye, F., Lyu, Y., Wang, X., Sugiyama, M., Zhang, Y., and Tsang, I. Sharpness-aware black-box optimization. *arXiv preprint arXiv:2410.12457*, 2024.

Yu, Q., Zhang, Z., Zhu, R., Yuan, Y., Zuo, X., Yue, Y., Dai, W., Fan, T., Liu, G., Liu, L., et al. Dapo: An open-source llm reinforcement learning system at scale. *arXiv preprint arXiv:2503.14476*, 2025.

Zheng, C., Liu, S., Li, M., Chen, X.-H., Yu, B., Gao, C., Dang, K., Liu, Y., Men, R., Yang, A., et al. Group sequence policy optimization. *arXiv preprint arXiv:2507.18071*, 2025.

Zhong, Q., Ding, L., Shen, L., Mi, P., Liu, J., Du, B., and Tao, D. Improving sharpness-aware minimization with fisher mask for better generalization on language models. *arXiv preprint arXiv:2210.05497*, 2022.

Ziegler, D. M., Stiennon, N., Wu, J., Brown, T. B., Radford, A., Amodei, D., Christiano, P., and Irving, G. Fine-tuning language models from human preferences. *arXiv preprint arXiv:1909.08593*, 2019.

A. Evolution Strategies

Algorithm 4 Evolution Strategies (ES)

Input: initial parameters θ_0 , reward function R , population size N , noise scale σ , learning rate α , iterations T
Output: model parameters θ_T

```

for  $t = 0$  to  $T - 1$  do
  for  $n = 1$  to  $N$  do
    Sample Gaussian noise  $\epsilon_n \sim \mathcal{N}(0, I)$ 
    Construct perturbed parameters  $\theta_t^{(n)} = \theta_t + \sigma \epsilon_n$ 
    Evaluate reward  $r_n = R(\theta_t^{(n)})$ 
  end for
  Compute mean  $\mu_r = \frac{1}{N} \sum_{n=1}^N r_n$ 
  Compute std  $s_r = \sqrt{\frac{1}{N} \sum_{n=1}^N (r_n - \mu_r)^2}$ 
  for  $n = 1$  to  $N$  do
    Normalize reward  $\hat{r}_n = \frac{r_n - \mu_r}{s_r + \varepsilon}$ 
  end for
  Update parameters  $\theta_{t+1} = \theta_t + \alpha \cdot \frac{1}{N} \sum_{n=1}^N \hat{r}_n \epsilon_n$ 
end for

```

Algorithm 4 presents the basic framework of using ES to fine-tune LLMs.

Specifically, Given a pretrained LLM with parameters θ_0 and a reward function $R(\theta)$, we aim to maximize the expected reward by iteratively updating model parameters. At iteration t , we sample N i.i.d. Gaussian noises $\epsilon_n \sim \mathcal{N}(0, I)$ for $n = 1, \dots, N$, and construct perturbed models:

$$\theta_t^{(n)} = \theta_t + \sigma \epsilon_n, \quad n = 1, \dots, N. \quad (18)$$

We evaluate each perturbed model to obtain reward scores:

$$r_n = R(\theta_t^{(n)}), \quad n = 1, \dots, N. \quad (19)$$

We then apply z-score normalization to keep the reward scale consistent:

$$\mu_r = \frac{1}{N} \sum_{n=1}^N r_n, \quad s_r = \sqrt{\frac{1}{N} \sum_{n=1}^N (r_n - \mu_r)^2}, \quad (20)$$

$$\hat{r}_n = \frac{r_n - \mu_r}{s_r + \varepsilon}, \quad n = 1, \dots, N, \quad (21)$$

where ε is a small constant for numerical stability. Finally, we update the parameters by aggregating perturbations weighted by normalized rewards:

$$\theta_{t+1} = \theta_t + \alpha \cdot \frac{1}{\sigma} \frac{1}{N} \sum_{n=1}^N \hat{r}_n \epsilon_n. \quad (22)$$

To reduce tuning complexity, we absorb $1/\sigma$ into the learning rate α . The update rule becomes:

$$\theta_{t+1} = \theta_t + \alpha \cdot \frac{1}{N} \sum_{n=1}^N \hat{r}_n \epsilon_n. \quad (23)$$

B. Proof

By the Taylor's expansion, we have

$$R(\theta + \sigma\epsilon_n) = R(\theta) + \sigma \langle \nabla R(\theta), \epsilon_n \rangle + \alpha(\theta, \sigma\epsilon_n), \quad (24)$$

where

$$\alpha(\theta, \sigma\epsilon_n) \triangleq R(\theta + \sigma\epsilon_n) - \left(R(\theta) + \sigma \langle \nabla R(\theta), \epsilon_n \rangle \right). \quad (25)$$

By the \mathcal{L} -smoothness, we can obtain that

$$\mathbb{E}[|\alpha(\theta, \sigma\epsilon_n)|] \leq \mathbb{E}\left[\frac{\mathcal{L}\sigma^2}{2} \|\epsilon_n\|^2\right] \leq \frac{(d+2)\mathcal{L}\sigma^2}{2}, \quad (26)$$

Lemma B.1. *Let the estimated variance s_r be defined in Eq. (9) Then it holds that*

$$\mathbb{E}[s_r^2] = \sigma^2 \|\nabla R(\theta)\|^2 + \zeta, \quad (27)$$

with

$$\begin{aligned} \zeta &= \mathbb{E}\left[\frac{1}{N-1} \sum_{i=1}^N \left(\alpha(\theta, \sigma\epsilon_i) - \frac{1}{N} \sum_{j=1}^N \alpha(\theta, \sigma\epsilon_j) \right)^2\right] \\ &\quad + \mathbb{E}\left[\frac{2\sigma}{N-1} \sum_{i=1}^N \left\langle \nabla R(\theta), \epsilon_i - \frac{1}{N} \sum_{j=1}^N \epsilon_j \right\rangle \left(\alpha(\theta, \sigma\epsilon_i) - \frac{1}{N} \sum_{j=1}^N \alpha(\theta, \sigma\epsilon_j) \right)\right]. \end{aligned}$$

Moreover,

$$|\zeta| \leq \frac{(d+2)^2 \mathcal{L}^2 \sigma^4}{4} + \frac{4N}{N-1} (d+1)^{\frac{1}{2}} (d+2) \mathcal{L} \sigma^3 \|\nabla R(\theta)\|. \quad (28)$$

Proof. First, we have

$$\begin{aligned} R(\theta + \sigma\epsilon_i) - \frac{1}{N} \sum_{j=1}^N R(\theta + \sigma\epsilon_j) &\stackrel{\text{Eq. (24)}}{=} R(\theta) + \sigma \langle \nabla R(\theta), \epsilon_i \rangle + \alpha(\theta, \sigma\epsilon_i) - \frac{1}{N} \sum_{j=1}^N \left(R(\theta) + \sigma \langle \nabla R(\theta), \epsilon_j \rangle + \alpha(\theta, \sigma\epsilon_j) \right) \\ &= \sigma \left\langle \nabla R(\theta), \epsilon_i - \frac{1}{N} \sum_{j=1}^N \epsilon_j \right\rangle + \alpha(\theta, \sigma\epsilon_i) - \frac{1}{N} \sum_{j=1}^N \alpha(\theta, \sigma\epsilon_j). \end{aligned} \quad (29)$$

Define

$$\beta_i \triangleq \alpha(\theta, \sigma\epsilon_i) - \frac{1}{N} \sum_{j=1}^N \alpha(\theta, \sigma\epsilon_j).$$

Then

$$\begin{aligned} \sum_{i=1}^N \left(R(\theta + \sigma\epsilon_i) - \frac{1}{N} \sum_{j=1}^N R(\theta + \sigma\epsilon_j) \right)^2 &= \sum_{i=1}^N \left(\sigma \left\langle \nabla R(\theta), \epsilon_i - \frac{1}{N} \sum_{j=1}^N \epsilon_j \right\rangle + \beta_i \right)^2 \\ &= \sum_{i=1}^N \left(\sigma^2 \left\langle \nabla R(\theta), \epsilon_i - \frac{1}{N} \sum_{j=1}^N \epsilon_j \right\rangle^2 + \beta_i^2 \right. \\ &\quad \left. + 2\sigma \left\langle \nabla R(\theta), \epsilon_i - \frac{1}{N} \sum_{j=1}^N \epsilon_j \right\rangle \beta_i \right). \end{aligned} \quad (30)$$

Furthermore, it holds that

$$\mathbb{E} \left[\sum_{i=1}^N \beta_i^2 \right] = \mathbb{E} \left[\left(1 - \frac{1}{N} \right) \sum_{i=1}^N \alpha^2(\theta, \sigma \epsilon_i) \right] \leq (N-1) \frac{\mathcal{L}^2 \sigma^4 (d+2)^2}{4}, \quad (31)$$

and

$$\begin{aligned} \mathbb{E} \left[\sum_{i=1}^N \left| \left\langle \nabla R(\theta), \epsilon_i - \frac{1}{N} \sum_{j=1}^N \epsilon_j \right\rangle \beta_i \right| \right] &\leq \mathbb{E} \left[N \left\| \left\langle \nabla R(\theta), \epsilon_i - \frac{1}{N} \sum_{j=1}^N \epsilon_j \right\rangle \right\| \|\beta_i\| \right] \\ &\stackrel{\text{Eq. (26)}}{\leq} 2N(d+1)^{\frac{1}{2}}(d+2)\mathcal{L}\sigma^2 \|\nabla R(\theta)\|. \end{aligned} \quad (32)$$

Therefore, we can obtain that

$$\begin{aligned} \mathbb{E}[s_r^2] &= \mathbb{E} \left[\frac{1}{N-1} \sum_{i=1}^N \left(\sigma^2 \left\langle \nabla R(\theta), \epsilon_i - \frac{1}{N} \sum_{j=1}^N \epsilon_j \right\rangle^2 + \beta_i^2 + 2\sigma \left\langle \nabla R(\theta), \epsilon_i - \frac{1}{N} \sum_{j=1}^N \epsilon_j \right\rangle \beta_i \right) \right] \\ &= \sigma^2 \|\nabla R(\theta)\|^2 + \zeta. \end{aligned} \quad (33)$$

Finally,

$$\begin{aligned} |\zeta| &\leq \mathbb{E} \left[\frac{1}{N-1} \sum_{i=1}^N \beta_i^2 + \frac{2\sigma}{N-1} \sum_{i=1}^N \left| \left\langle \nabla R(\theta), \epsilon_i - \frac{1}{N} \sum_{j=1}^N \epsilon_j \right\rangle \beta_i \right| \right] \\ &\leq \frac{(d+2)^2 \mathcal{L}^2 \sigma^4}{4} + \frac{4N}{N-1} (d+1)^{\frac{1}{2}}(d+2)\mathcal{L}\sigma^3 \|\nabla R(\theta)\|. \end{aligned} \quad (34)$$

□

Lemma B.2. Let the stochastic gradient estimation g_t be defined in Eq. (8) Then its norm satisfies

$$\mathbb{E}[\|g_t\|^2] = \frac{N^3 + (d-2)N^2 + (3-2d)N + d-2}{N^3} \|\nabla R(\theta)\|^2 + \gamma, \quad (35)$$

with

$$\begin{aligned} \gamma &= \mathbb{E} \left[\frac{1}{\sigma^2} \frac{1}{N^2} \left(\sum_{n=1}^N \alpha(\theta, \sigma \epsilon_n) \epsilon_n \right)^2 + \frac{1}{\sigma^2} \frac{1}{N^4} \left(\sum_{n=1}^N \sum_{i=1}^N \alpha(\theta, \sigma \epsilon_i) \epsilon_n \right)^2 \right. \\ &\quad - 2 \frac{1}{\sigma^2} \frac{1}{N^3} \left(\sum_{n=1}^N \alpha(\theta, \sigma \epsilon_n) \epsilon_n \right)^\top \left(\sum_{n=1}^N \sum_{i=1}^N \alpha(\theta, \sigma \epsilon_i) \epsilon_n \right) \\ &\quad \left. + 2 \left\langle \frac{1}{N} \sum_{n=1}^N \epsilon_n \epsilon_n^\top \nabla R(\theta) - \frac{1}{N^2} \sum_{n=1}^N \sum_{i=1}^N \langle \nabla R(\theta), \epsilon_i \rangle \epsilon_n, \frac{1}{\sigma} \frac{1}{N} \sum_{n=1}^N \alpha(\theta, \sigma \epsilon_n) \epsilon_n - \frac{1}{\sigma} \frac{1}{N^2} \sum_{n=1}^N \sum_{i=1}^N \alpha(\theta, \sigma \epsilon_i) \epsilon_n \right\rangle \right]. \end{aligned} \quad (36)$$

Furthermore, it holds that

$$|\gamma| \leq \frac{(d+2)^2 \mathcal{L}^2 \sigma^2}{N} + \frac{4(d+2)\mathcal{L}\sigma}{N} \|\nabla R(\theta)\|. \quad (37)$$

Proof. First, we have

$$g_t = \frac{1}{N} \sum_{n=1}^N \epsilon_n \epsilon_n^\top \nabla R(\theta) - \frac{1}{N^2} \sum_{i=1}^N \sum_{j=1}^N \langle \nabla R(\theta), \epsilon_j \rangle \epsilon_i + \frac{1}{\sigma} \frac{1}{N} \sum_{n=1}^N \alpha(\theta, \sigma \epsilon_n) \epsilon_n - \frac{1}{\sigma} \frac{1}{N^2} \sum_{n=1}^N \sum_{i=1}^N \alpha(\theta, \sigma \epsilon_i) \epsilon_n \quad (38)$$

Thus,

$$\begin{aligned} \mathbb{E}[g_t] &= \mathbb{E}\left[\frac{1}{N} \sum_{n=1}^N \epsilon_n \epsilon_n^\top \nabla R(\theta) - \frac{1}{N^2} \sum_{i=1}^N \sum_{j=1}^N \langle \nabla R(\theta), \epsilon_j \rangle \epsilon_i\right] + \mathbb{E}\left[\frac{1}{\sigma} \frac{1}{N} \sum_{n=1}^N \alpha(\theta, \sigma \epsilon_n) \epsilon_n - \frac{1}{\sigma} \frac{1}{N^2} \sum_{n=1}^N \sum_{i=1}^N \alpha(\theta, \sigma \epsilon_i) \epsilon_n\right] \\ &= \frac{N-1}{N} \nabla R(\theta) + \tau \end{aligned} \quad (39)$$

$$|\tau| = \mathbb{E}\left[\frac{1}{\sigma} \frac{1}{N} \sum_{n=1}^N \alpha(\theta, \sigma \epsilon_n) \epsilon_n - \frac{1}{\sigma} \frac{1}{N^2} \sum_{n=1}^N \sum_{i=1}^N \alpha(\theta, \sigma \epsilon_i) \epsilon_n\right] \leq \mathcal{L} \sigma (d+2) \quad (40)$$

Define

$$A \triangleq \frac{1}{N} \sum_{n=1}^N \epsilon_n \epsilon_n^\top \nabla R(\theta) - \frac{1}{N^2} \sum_{i=1}^N \sum_{j=1}^N \langle \nabla R(\theta), \epsilon_j \rangle \epsilon_i, B \triangleq \frac{1}{\sigma} \frac{1}{N} \sum_{n=1}^N \alpha(\theta, \sigma \epsilon_n) \epsilon_n - \frac{1}{\sigma} \frac{1}{N^2} \sum_{n=1}^N \sum_{i=1}^N \alpha(\theta, \sigma \epsilon_i) \epsilon_n. \quad (41)$$

$$\begin{aligned} \|g_t\|^2 &= \left\| \frac{1}{N} \sum_{n=1}^N \epsilon_n \epsilon_n^\top \nabla R(\theta) - \frac{1}{N^2} \sum_{i=1}^N \sum_{j=1}^N \langle \nabla R(\theta), \epsilon_j \rangle \epsilon_i \right\|^2 \\ &\quad + \left\| \frac{1}{\sigma} \frac{1}{N} \sum_{n=1}^N \alpha(\theta, \sigma \epsilon_n) \epsilon_n - \frac{1}{\sigma} \frac{1}{N^2} \sum_{n=1}^N \sum_{i=1}^N \alpha(\theta, \sigma \epsilon_i) \epsilon_n \right\|^2 \\ &\quad + 2 \left\langle \frac{1}{N} \sum_{n=1}^N \epsilon_n \epsilon_n^\top \nabla R(\theta) - \frac{1}{N^2} \sum_{n=1}^N \sum_{i=1}^N \langle \nabla R(\theta), \epsilon_i \rangle \epsilon_n, \frac{1}{\sigma} \frac{1}{N} \sum_{n=1}^N \alpha(\theta, \sigma \epsilon_n) \epsilon_n - \frac{1}{\sigma} \frac{1}{N^2} \sum_{n=1}^N \sum_{i=1}^N \alpha(\theta, \sigma \epsilon_i) \epsilon_n \right\rangle. \end{aligned} \quad (42)$$

Then

$$\begin{aligned} \|A\|^2 &= \frac{1}{N^2} \sum_{i=1}^N \sum_{j=1}^N \langle \epsilon_i \epsilon_i^\top \nabla R(\theta), \epsilon_j \epsilon_j^\top \nabla R(\theta) \rangle + \frac{1}{N^4} \sum_{i=1}^N \sum_{j=1}^N \sum_{k=1}^N \sum_{l=1}^N \langle \langle \nabla R(\theta), \epsilon_i \rangle \epsilon_j, \langle \nabla R(\theta), \epsilon_k \rangle \epsilon_l \rangle \\ &\quad - \frac{2}{N^3} \left\langle \sum_{n=1}^N \epsilon_n \epsilon_n^\top \nabla R(\theta), \sum_{i=1}^N \sum_{j=1}^N \langle \nabla R(\theta), \epsilon_i \rangle \epsilon_j \right\rangle. \end{aligned} \quad (43)$$

$$\begin{aligned} \mathbb{E}\left[\|A\|^2\right] &= \frac{N+d}{N} \|\nabla R(\theta)\|^2 + \frac{3(N-1)+d+1}{N^3} \|\nabla R(\theta)\|^2 - \frac{2(N+d)}{N^2} \|\nabla R(\theta)\|^2 \\ &= \frac{N^3 + (d-2)N^2 + (3-2d)N + d - 2}{N^3} \|\nabla R(\theta)\|^2 \end{aligned} \quad (44)$$

$$\begin{aligned}\|B\|^2 &= \frac{1}{\sigma^2} \frac{1}{N^2} \left\| \sum_{n=1}^N \alpha(\theta, \sigma \epsilon_n) \epsilon_n \right\|^2 + \frac{1}{\sigma^2} \frac{1}{N^4} \left\| \sum_{n=1}^N \sum_{i=1}^N \alpha(\theta, \sigma \epsilon_i) \epsilon_n \right\|^2 \\ &\quad - 2 \frac{1}{\sigma^2} \frac{1}{N^3} \left(\sum_{n=1}^N \alpha(\theta, \sigma \epsilon_n) \epsilon_n \right)^\top \left(\sum_{n=1}^N \sum_{i=1}^N \alpha(\theta, \sigma \epsilon_i) \epsilon_n \right).\end{aligned}\quad (45)$$

$$\left\langle A, B \right\rangle = \left\langle \frac{1}{N} \sum_{n=1}^N \epsilon_n \epsilon_n^\top \nabla R(\theta) - \frac{1}{N^2} \sum_{n=1}^N \sum_{i=1}^N \langle \nabla R(\theta), \epsilon_i \rangle \epsilon_n, \frac{1}{\sigma} \frac{1}{N} \sum_{n=1}^N \alpha(\theta, \sigma \epsilon_n) \epsilon_n - \frac{1}{\sigma} \frac{1}{N^2} \sum_{n=1}^N \sum_{i=1}^N \alpha(\theta, \sigma \epsilon_i) \epsilon_n \right\rangle. \quad (46)$$

$$\gamma = \mathbb{E} \left[\|B\|^2 \right] + 2\mathbb{E} \left[\left\langle A, B \right\rangle \right] \quad (47)$$

Thus,

$$\begin{aligned}\mathbb{E} [\|g_t\|^2] &= \mathbb{E} [\|A\|^2] + \mathbb{E} [\|B\|^2] + 2\mathbb{E} \left[\left\langle A, B \right\rangle \right] \\ &= \frac{N^3 + (d-2)N^2 + (3-2d)N + d-2}{N^3} \|\nabla R(\theta)\|^2 + \gamma\end{aligned}\quad (48)$$

There are also,

$$\mathbb{E} [\|B\|^2] \leq \frac{\mathcal{L}^2 \sigma^2 (d+2)^2}{4N} + \frac{\mathcal{L}^2 \sigma^2 (d+2)^2}{4N} + \frac{\mathcal{L}^2 \sigma^2 (d+2)^2}{2N} = \frac{\mathcal{L}^2 \sigma^2 (d+2)^2}{N} \quad (49)$$

$$\begin{aligned}\mathbb{E} \left[\left\langle A, B \right\rangle \right] &\leq \frac{\mathcal{L} \sigma (d+2)}{2N} \|\nabla R(\theta)\| + \frac{\mathcal{L} \sigma (d+2)}{2N} \|\nabla R(\theta)\| + \frac{\mathcal{L} \sigma (d+2)}{2N} \|\nabla R(\theta)\| + \frac{\mathcal{L} \sigma (d+2)}{2N} \|\nabla R(\theta)\| \\ &= \frac{2\mathcal{L} \sigma (d+2)}{N} \|\nabla R(\theta)\|\end{aligned}\quad (50)$$

Finally,

$$|\gamma| \leq \frac{(d+2)^2 \mathcal{L}^2 \sigma^2}{N} + \frac{4(d+2) \mathcal{L} \sigma}{N} \|\nabla R(\theta)\|. \quad (51)$$

□

B.1. Proof of Proposition 3.1

Proof. From Lemma B.1 and Lemma B.2, we know

$$\mathbb{E} [\|g_t\|^2] = \frac{N^3 + (d-2)N^2 + (3-2d)N + d-2}{N^3} \|\nabla R(\theta)\|^2 + \gamma, \quad \gamma = O(\sigma), \quad (52)$$

$$\mathbb{E} [s_r^2] = \sigma^2 \|\nabla R(\theta)\|^2 + \zeta, \quad \zeta = O(\sigma^3). \quad (53)$$

Comparing Eq. 52 and Eq. 53, and ignoring the perturbation terms ζ and γ (which are higher-order terms with respect to σ), we can obtain that:

$$\mathbb{E}[\|g_t\|^2] = \frac{N^3 + (d-2)N^2 + (3-2d)N + d - 2}{N^3} \cdot \sigma^{-2} \cdot \mathbb{E}[s_r^2]. \quad (54)$$

□

C. Hyperparameter Settings

For all ES and ESSAM experiments, we set the hyperparameter $\rho = 10^{-4}$ and the learning rate $\alpha = 2.5 \times 10^{-4}$. The population size N and the noise scale σ are chosen as shown in Table 3. For the PPO and GRPO experiments, we set the learning rate α and the KL-divergence penalty coefficient β as shown in Table 4. In addition, for the GRPO experiments, we set the group size to $N = 8$.

Table 3. Hyperparameter settings for ES and ESSAM across different models. Each pair (\cdot, \cdot) denotes (population size N , noise scale σ); the symbol \checkmark indicates the hyperparameter setting for each model-method combination.

METHOD	MODEL	$(40, 1.5 \times 10^{-3})$	$(40, 2 \times 10^{-3})$	$(60, 1.5 \times 10^{-3})$	$(60, 2 \times 10^{-3})$
ES	QWEN-0.5B-INSTRUCT	✓			
	QWEN-1.5B-INSTRUCT			✓	
	QWEN-3B-INSTRUCT		✓		
	QWEN-7B-INSTRUCT				✓
	LLAMA-1B-INSTRUCT	✓			
	LLAMA-3B-INSTRUCT				✓
	LLAMA-8B-INSTRUCT				✓
ESSAM	QWEN-0.5B-INSTRUCT	✓			
	QWEN-1.5B-INSTRUCT			✓	
	QWEN-3B-INSTRUCT		✓		
	QWEN-7B-INSTRUCT				✓
	LLAMA-1B-INSTRUCT	✓			
	LLAMA-3B-INSTRUCT				✓
	LLAMA-8B-INSTRUCT				✓

Table 4. Hyperparameter settings for PPO and GRPO across different models. Each pair (\cdot, \cdot) denotes (learning rate α , KL-divergence penalty coefficient β); the symbol \checkmark indicates the hyperparameter setting for each model-method combination.

METHOD	MODEL	$(10^{-6}, 10^{-3})$	$(10^{-5}, 10^{-3})$	$(10^{-6}, 5 \times 10^{-3})$	$(10^{-5}, 5 \times 10^{-3})$
PPO	QWEN-0.5B-INSTRUCT	✓			
	QWEN-1.5B-INSTRUCT	✓			
	QWEN-3B-INSTRUCT	✓			
	QWEN-7B-INSTRUCT		✓		
	LLAMA-1B-INSTRUCT	✓			
	LLAMA-3B-INSTRUCT				✓
	LLAMA-8B-INSTRUCT			✓	
GRPO	QWEN-0.5B-INSTRUCT	✓			
	QWEN-1.5B-INSTRUCT	✓			
	QWEN-3B-INSTRUCT	✓			
	QWEN-7B-INSTRUCT	✓			
	LLAMA-1B-INSTRUCT				✓
	LLAMA-3B-INSTRUCT		✓		
	LLAMA-8B-INSTRUCT	✓			

D. Detailed GPU Memory Usage

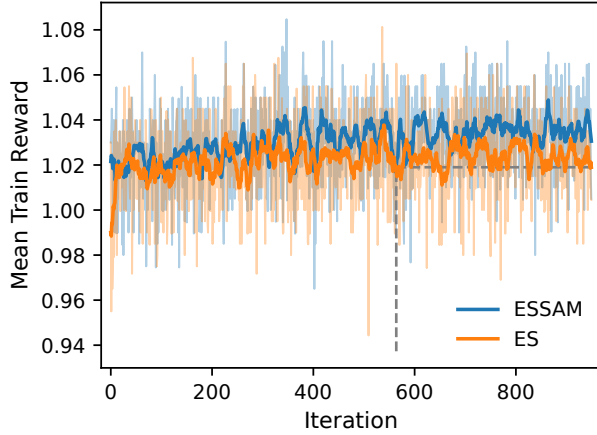
Table 5 shows the detailed GPU memory usage when fine-tuning different LLMs with different algorithms.

Table 5. The detailed GPU memory usage.

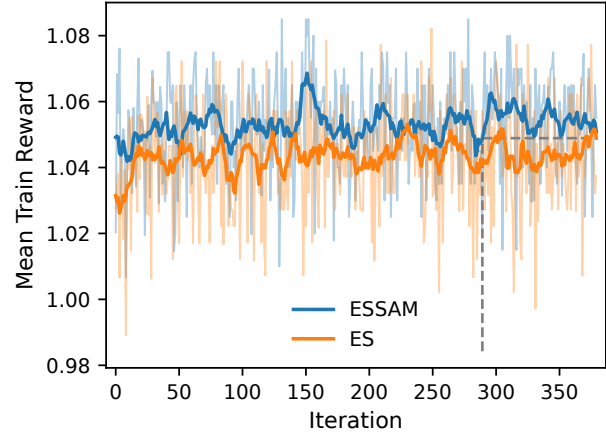
BASE MODEL	RL		ES	ESSAM
	PPO	GRPO		
QWEN-2.5-0.5B-INSTRUCT	57.32	34.20	2.99	2.99
QWEN-2.5-1.5B-INSTRUCT	123.40	70.80	6.57	6.57
QWEN-2.5-3B-INSTRUCT	208.96	102.24	9.96	9.96
QWEN-2.5-7B-INSTRUCT	314.40	212.88	19.85	19.85
LLAMA-3.2-1B-INSTRUCT	99.20	65.68	4.90	4.90
LLAMA-3.2-3B-INSTRUCT	201.24	92.60	11.49	11.49
LLAMA-3.1-8B-INSTRUCT	314.44	219.48	21.45	21.45

E. Training Reward Curve

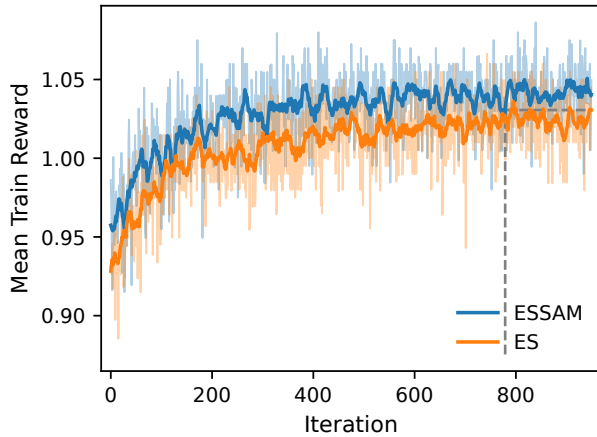
As shown in Figure 7, we present the curves of the evolution of the average training reward for more models fine-tuned with ES and ESSAM.



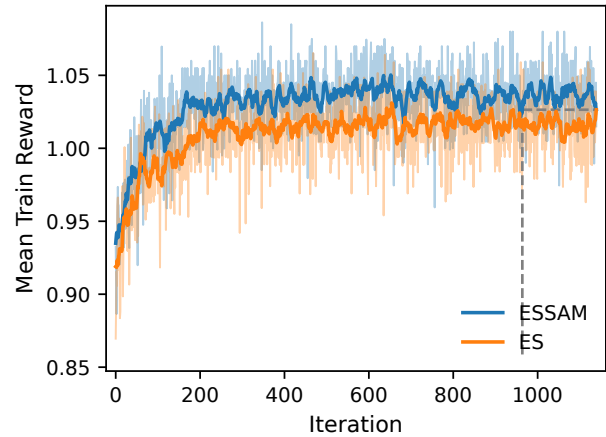
(a) Qwen-2.5-3B-Instruct



(b) Qwen-2.5-7B-Instruct



(c) LLaMA-3.2-3B-Instruct



(d) LLaMA-3.1-8B-Instruct

Figure 7. The training mean reward curves of ESSAM and ES.

F. Test Set Accuracy

As shown in Figure 8, we present schematic diagrams of the evolution of test set accuracy for more models fine-tuned with different algorithms.

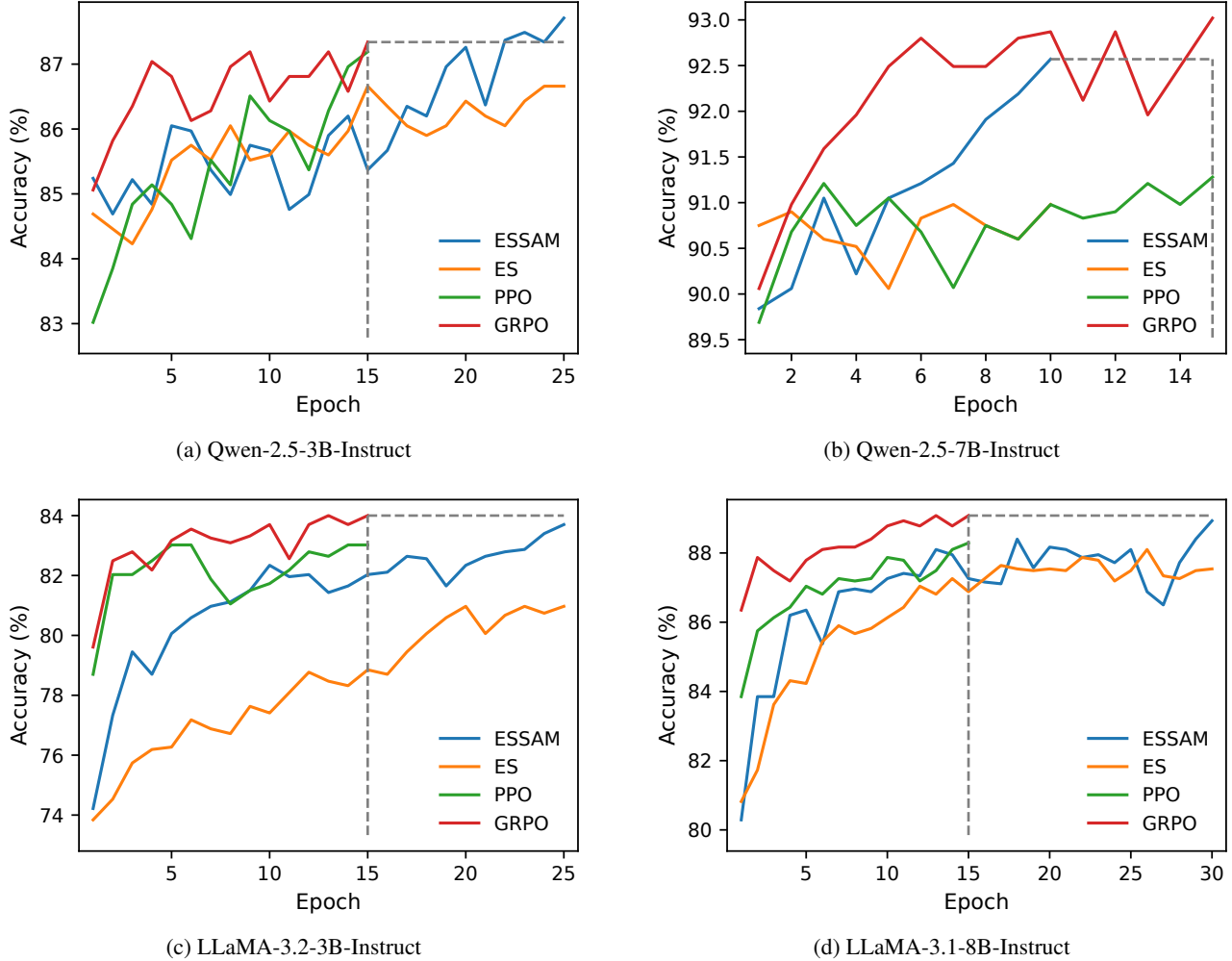


Figure 8. A schematic illustration of how the test set accuracy of models fine-tuned with different algorithms evolves over training.

G. Example

In this section, we present example responses from models fine-tuned with ESSAM.

Qwen2.5-0.5b-Instruct

Prompt: You are a helpful assistant. You first think about the reasoning process in your mind and then provide the user with the answer. Please solve the following problem: A robe takes 2 bolts of blue fiber and half that much white fiber. How many bolts in total does it take? Show your work in `<think>` `</think>` tags. And put the final numerical answer after `###`.

Model Response: Let me solve this step by step. *<think>* First, we know that the robe takes 2 bolts of blue fiber. According to the problem, the white fiber is half the amount of blue fiber. So, the white fiber is $\frac{2}{2} = 1$ bolt. Therefore, the total number of bolts needed for the robe is the sum of the blue and white fibers, which is $2 + 1 = 3$ bolts. *<think> ##### 3*

Qwen2.5-1.5b-Instruct

Prompt: You are a helpful assistant. You first think about the reasoning process in your mind and then provide the user with the answer. Please solve the following problem: Janet's ducks lay 16 eggs per day. She eats three for breakfast every morning and bakes muffins for her friends every day with four. She sells the remainder at the farmers' market daily for \$2 per fresh duck egg. How much in dollars does she make every day at the farmers' market? Show your work in *<think> </think>* tags. And put the final numerical answer after #####.

Model Response: Let me solve this step by step. *<think>* First, let's determine the total number of eggs laid by Janet's ducks per day. Janet's ducks lay 16 eggs per day. Janet eats 3 eggs for breakfast every morning. So, the number of eggs left after breakfast is $16 - 3 = 13$ eggs. Next, she bakes muffins for her friends with 4 eggs. So, the number of eggs left after baking muffins is $13 - 4 = 9$ eggs. These 9 eggs are sold at the farmers' market. Each egg is sold for \$2. Therefore, the total amount of money she makes from selling the eggs is $9 \times 2 = 18$ dollars. *<think> ##### 18*

Qwen2.5-3b-Instruct

Prompt: You are a helpful assistant. You first think about the reasoning process in your mind and then provide the user with the answer. Please solve the following problem: Every day, Wendi feeds each of her chickens three cups of mixed chicken feed, containing seeds, mealworms and vegetables to help keep them healthy. She gives the chickens their feed in three separate meals. In the morning, she gives her flock of chickens 15 cups of feed. In the afternoon, she gives her chickens another 25 cups of feed. How many cups of feed does she need to give her chickens in the final meal of the day if the size of Wendi's flock is 20 chickens? Show your work in *<think> </think>* tags. And put the final numerical answer after #####.

Model Response: Let me solve this step by step. *<think>* First, we need to determine the total amount of feed Wendi gives to her chickens in a day. We know that each chicken gets 3 cups of feed per day. Wendi has a flock of 20 chickens.

So, the total feed given to the chickens in a day is:

$$20 \text{ chickens} \times 3 \text{ cups/chicken} = 60 \text{ cups}$$

Next, we need to account for the feed given in the morning and the afternoon. Wendi gives 15 cups in the morning and 25 cups in the afternoon.

So, the total feed given in the morning and afternoon is:

$$15 \text{ cups} + 25 \text{ cups} = 40 \text{ cups}$$

To find out how much feed is needed for the final meal, we subtract the feed given in the morning and afternoon from the total daily feed:

$$60 \text{ cups} - 40 \text{ cups} = 20 \text{ cups}$$

Therefore, the amount of feed needed for the final meal is 20 cups. *<think> ##### 20*

Qwen2.5-7b-Instruct

Prompt: You are a helpful assistant. You first think about the reasoning process in your mind and then provide the user with the answer. Please solve the following problem: Josh decides to try flipping a house. He buys a house for \$80,000 and then puts in \$50,000 in repairs. This increased the value of the house by 150%. How much profit did he make? Show your work in `<think> </think>` tags. And put the final numerical answer after `####`.

Model Response: Let me solve this step by step. `<think>` First, we need to calculate the new value of the house after the repairs. The original value of the house was \$80,000, and the repairs increased the value by 150%. The increase in value due to repairs is:

$$80,000 \times 1.50 = 120,000$$

So, the new value of the house is:

$$80,000 + 120,000 = 200,000$$

Next, we need to calculate the total cost Josh incurred. This includes the purchase price of the house and the repair costs:

$$80,000 + 50,000 = 130,000$$

Now, we can find the profit by subtracting the total cost from the new value of the house:

$$200,000 - 130,000 = 70,000$$

So, the profit Josh made is \$70,000. `<think> #### 70000`

LLaMA-3.2-1B-Instruct

Prompt: You are a helpful assistant. You first think about the reasoning process in your mind and then provide the user with the answer. Please solve the following problem: James decides to run 3 sprints 3 times a week. He runs 60 meters each sprint. How many total meters does he run a week? Show your work in `<think> </think>` tags. And put the final numerical answer after `####`.

Model Response: Let me solve this step by step. `<think>` Step 1: Calculate the total number of sprints per week

James decides to run 3 sprints 3 times a week, so the total number of sprints per week is:

$$3 \text{ sprints} \times 3 \text{ times} = 9 \text{ sprints}$$

Step 2: Calculate the total meters run per sprint

Each sprint is 60 meters.

Step 3: Calculate the total meters run per week

To find the total meters run per week, multiply the total number of sprints per week by the meters run per sprint:

$$9 \text{ sprints} \times 60 \text{ meters/sprint} = 540 \text{ meters}$$

`<think> #### 540`

LLaMA-3.2-3B-Instruct

Prompt: You are a helpful assistant. You first think about the reasoning process in your mind and then provide the user with the answer. Please solve the following problem: Toulouse has twice as many sheep as Charleston.

Charleston has 4 times as many sheep as Seattle. How many sheep do Toulouse, Charleston, and Seattle have together if Seattle has 20 sheep? Show your work in `<think> </think>` tags. And put the final numerical answer after `####`.

Model Response: Let me solve this step by step. `<think>` First, let's determine the number of sheep Charleston has. Since Charleston has 4 times as many sheep as Seattle, and Seattle has 20 sheep. So, the number of sheep Charleston has is:

$$4 \times 20 = 80 \text{ sheep}$$

Next, let's determine the number of sheep Toulouse has. Since Toulouse has twice as many sheep as Charleston, and Charleston has 80 sheep.

So, the number of sheep Toulouse has is:

$$2 \times 80 = 160 \text{ sheep}$$

Now, let's add up the number of sheep all three cities have together. Seattle has 20 sheep, Charleston has 80 sheep, and Toulouse has 160 sheep.

So, the total number of sheep is:

$$20 + 80 + 160 = 260 \text{ sheep}$$

`<think> #### 260`

LLaMA-3.1-8B-Instruct

Prompt: You are a helpful assistant. You first think about the reasoning process in your mind and then provide the user with the answer. Please solve the following problem: John drives for 3 hours at a speed of 60 mph and then turns around because he realizes he forgot something very important at home. He tries to get home in 4 hours but spends the first 2 hours in standstill traffic. He spends the next half-hour driving at a speed of 30mph, before being able to drive the remaining time of the 4 hours going at 80 mph. How far is he from home at the end of those 4 hours? Show your work in `<think> </think>` tags. And put the final numerical answer after `####`.

Model Response: Let me solve this step by step. `<think>` Step 1: Calculate the distance John drives for the first 3 hours at 60 mph. Distance = Speed \times Time, so the distance is:

$$60 \text{ mph} \times 3 \text{ hours} = 180 \text{ miles}$$

So, John is 180 miles away from home after driving for 3 hours.

Step 2: Since John turns around and tries to get home in 4 hours, we need to calculate the distance he covers in those 4 hours. However, he spends the first 2 hours in standstill traffic, which means he doesn't move at all during those 2 hours. So, for the first 2 hours, the distance covered is:

$$0 \text{ miles}$$

Step 3: Then, he spends the next half-hour (0.5 hours) driving at a speed of 30 mph. Distance = Speed \times Time, so the distance covered is:

$$30 \text{ mph} \times 0.5 \text{ hours} = 15 \text{ miles}$$

So, in the next half-hour, he covers 15 miles.

Step 4: After the half-hour of driving at 30 mph, he has 1.5 hours left to reach his goal of getting home in 4 hours. During these remaining 1.5 hours, he drives at a speed of 80 mph. Distance = Speed \times Time, so the distance covered is:

$$80 \text{ mph} \times 1.5 \text{ hours} = 120 \text{ miles}$$

So, in the last 1.5 hours, he covers 120 miles.

Step 5: Now, let's calculate the total distance he covers in the 4 hours to get back home. Distance covered in the first 2 hours of standstill traffic = 0 miles

Distance covered in the next half-hour at 30 mph = 15 miles

Distance covered in the last 1.5 hours at 80 mph = 120 miles

Total distance covered is:

$$0 + 15 + 120 = 135 \text{ miles}$$

Since John was initially 180 miles away from home and he covers a total distance of 135 miles to get back home, we need to calculate the remaining distance:

$$180 \text{ miles} - 135 \text{ miles} = 45 \text{ miles}$$

Therefore, John is 45 miles away from home at the end of those 4 hours. <think> ##### 45.